Particle Identification and Its Efficiency for Small Angle GDH Experiment in JLab Hall-A *

LÜ Hai-Jiang[1,2;1)] YE Yun-Xiu[1] YAN Xin-Hu[1] JIANG Yi[1] ZHANG Pei[1] YE Qiu-Jian[1]

1 (Department of Modern Physics, University of Science and Technology of China, Hefei 230026, China)
2 (Department of Physics, Huangshan University, Huangshan 245021, China)

Abstract To obtain a pure electron sample with high statistics, which is necessary for the asymmetry and cross section analysis for the small angle GDH experiment in JLab Hall-A, the information in shower and gas Cerenkov has been used in the particle identification. Due to the dependence of the kinematics, the PID cut and the corresponding efficiency have been optimized for different runs.

Key words GDH sum rule, particle identification, efficiency, optimization

1 Introduction

The Gerasimov-Drell-Hearn(GDH) sum rule[1, 2] applied to nuclei relates the total cross section of circularly polarized photons on a longitudinally polarized nucleus to the anomalous magnetic moment of the nucleus:

$$\int_{\rm thr}^{\infty}(\sigma_{\rm A}(\nu,Q^2)-\sigma_{\rm P}(\nu,Q^2))\frac{{\rm d}\nu}{\nu}=-4\pi^2\frac{\mu_{\rm A}^2}{J}\ , \qquad (1)$$

where $Q^2=-(k-k')^2$ is the negative four momentums square of the exchanged photon, k and k' are the four momentums of the incoming and scattering electron, respectively. $\sigma_{\rm P}$ and $\sigma_{\rm A}$ are the total photo-absorption cross sections on nucleus, with nuclear spin J parallel and antiparallel to the photon polarization, $\mu_{\rm A}=\mu-Jq\bar{h}/M$ is the anomalous magnetic moment of the nucleus, where q and M are the charge and mass of the nucleus. The lower limit is the photo-nuclear disintegration threshold.

The difficulty associated with the real photon experiments is that to measure the total absorption cross section, one needs to detect particles at all the solid angles, which is often not possible due to the incomplete coverage of the detectors. Inclusive electron scattering would be an attractive alternative method to measure the GDH sum rule, it proves one can measure at very low Q^2 and extrapolate to $Q^2=0$. The extrapolation will be reasonable if the slope of the GDH sum at the $Q^2=0$ point is smooth and can be measured.

There are some data at very low Q^2 range from 0.01 to 0.5$({\rm GeV}/c)^2$ with the polarized electron scattering of polarized ^{3}He by using the JLab Hall-A septum magnets[3], with which the Q^2 dependence of the GDH sum rule can be studied at this low Q^2 range. The slope of the GDH sum rule at Q^2 near zero can be measured and a reasonable extrapolation to the real photon point might be obtained.

To obtain the Q^2 dependence of the GDH sum rule, the cross section and cross section asymmetry for the scattering have to be measured. So the electron should be separated from the background particles, which are particles produced by reactions other than $({\rm ep}\rightarrow {\rm e'p})$ scattering. During this experiment

Received 4 January 2007
* Supported by National Natural Science Foundation of China (10605022) and National Science Foundation of Anhui Educational Committee (KJ2007B028)
1) E-mail: luhj9404@mail.ustc.edu.cn

the background mainly came from pions resulting from pion photo-production. The particle identification (PID) for this experiment was accomplished by a CO_2 threshold gas Cerenkov detector and a double-layered shower counter, which were called the pre-shower and the total-shower.

Since the information in shower counter depended on the kinematic of the particles[4], a same cut would lead to different cut efficiencies for different kinematic runs. To decrease the statistic uncertainty in this experiment, a high electron acceptance efficiency was required. One had to select different PID cuts for this requirement.

The PID efficiency was characterized by electron acceptance efficiency $\varepsilon_{\rm e}$ and pion rejection factor η_π, where $\varepsilon_{\rm e}$ was defined as the ratio of the number of electrons that were identified by the detector and the total number of electrons that entered the detector, η_π was defined as the ratio of the number of pions that were rejected and the total number of pions that entered the detector.

2 Particle identification

PID could be achieved by the Cerenkov detector and shower counter with two methods. One was to combine the information in two detectors for the PID. Another one was to use the independent cuts on the information in Cerenkov detector and shower counter. The former one was expected to have a higher electron acceptance efficiency and pion rejection factor. But one couldn't obtain pure electron or pion samples without the Cerenkov detector or shower counter at GDH experiment. The efficiency of the combined method depended on the simulation. This method was not so ideal since it was hard to fully describe the detectors in the real situation at JLab Hall-A. Because the particle identification of Cerenkov detector and shower counter was based on different mechanisms, the cut efficiencies of these two detectors were not correlated. We therefore used the cut based analysis to extract the PID efficiency of shower counter by using the sample selected by the Cerenkov detector, and vice versa. As the efficiency of shower cut depended on the particle kinematics, the shower cut should be optimized.

2.1 Performance of the gas Cerenkov detector

The threshold gas Cerenkov detector for the GDH experiment was filled with CO_2 at atmospheric pressure whose refraction index was 1.00041. The threshold speed and momentum were

$$v=\frac{c}{n},\quad p=\frac{mc}{\sqrt{n^2-1}}\ . \tag{2}$$

So the threshold momentums for electron and pion were about 18MeV/c and 4.9GeV/c, respectively. The acceptance momentum range for the JLab Hall-A spectrometer was from 0.3 to 4.0GeV. Thus the electrons could emit Cerenkov light and trigger an ADC signal but pions couldn't do that directly. The latter could interact with the matter it passed through and generated δ electron. The δ electrons would emit Cerenkov light and trigger the ADCs. But the δ electrons in general did not move in the same direction as the scattered electrons, so the Cerenkov light emitted by δ electrons would not be efficiently collected by the mirrors. The ADC signals generated by δ electrons were mostly in single photo-electron peak[4] and the ones from the scattering electrons were mostly in multi-electron peak.

The single photo-electron peak was scaled to 200 after the calibration correction for the Cerenkov detector[5]. One could separate the electrons from pions with the cut on the sum of ADC($\sum_{\rm ADC}$), the total signals in the Cerenkov detector.

The information of deposit energies in the pre-shower counter and the total-shower counter might help to provide a clean electron sample and pion sample for the optimization of the PID cuts in the Cerenkov detector. Fig. 1(a) shows a scattering plot of $E_{\rm ps}/p$ vs. $E_{\rm sh}/p$ for one particular kinematic run in 1992, where p is the momentum of the charged track, $E_{\rm ps}$ and $E_{\rm sh}$ are the corresponded energy deposit in the pre-shower and the total-shower counter. As shown in Fig. 1(b), the pion sample is selected by the requirements of $0.2<E_{\rm sh}/p<0.4$ and $0.03<E_{\rm ps}/p<0.09$. The electron sample must satisfy the requirement of $0.95<E/p<1.05$ and $0.3<E_{\rm ps}/p<0.6$, where $E=E_{\rm ps}+E_{\rm sh}$, the total deposit energy in the

shower counter. The $\sum_{\rm ADC}$ for pions and electrons are drawn in Fig. 1(c). The variation of electron acceptance efficiency $\varepsilon_{\rm e}^{\rm cer}$ and pion rejection rate $\eta_{\pi}^{\rm cer}$ in different $\sum_{\rm ADC}$ cuts could be obtained from the above samples. The results are shown in Fig. 2.

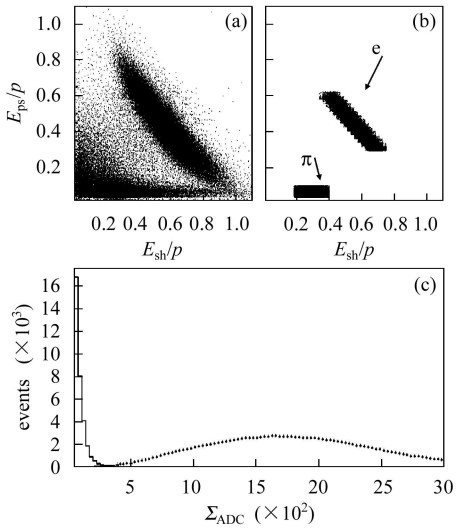

Fig. 1. (a) $E_{\rm ps}/p$ vs. $E_{\rm sh}/p$ scattering plot; (b) π and e samples; (c) Their summed ADC signals $\sum_{\rm ADC}$ in Cerenkov detector, the histogram and error bars are $\sum_{\rm ADC}$ of π and e samples, respectively.

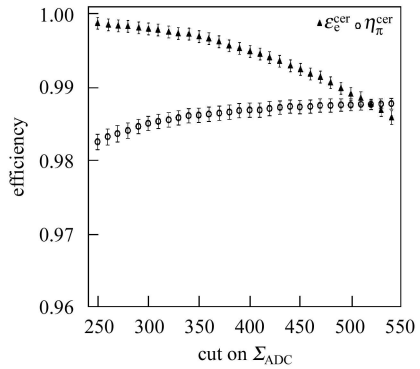

Fig. 2. Performance of gas Cerenkov: $\eta_{\pi}^{\rm cer}$ and $\varepsilon_{\rm e}^{\rm cer}$ with different cut values on $\sum_{\rm ADC}$. The statistical uncertainty is represent by the error bar.

2.2 Performance of the shower counter

In the kinematic range of this experiment, the negatively charged pion could masquerade as an electron in the detectors and should be rejected. The Cerenkov detector provides the primary method of separating pions from electron, but their characteristic signals in the shower counter could also be used to tag pions in the data.

The deposit energies in the pre-shower and total-shower counter could be applied to reject the pions and other low energy background events, which was illustrated in Fig. 3(a). The ratio of E/p was useful to separate the electrons and pions. It distributed around 1 for electrons and 0.3 for pions with the shower counter calibration[6]. The cluster began in the pre-sower counter and expanded in the total-shower counter when one particle passed through the calorimeter. Usually, the ratio of $E_{\rm ps}/p$ for most of pions was not more than 10 percent, but for electrons it might be in several ten percent. Pion could be separated from electrons by using the cut on $E_{\rm ps}/p$. The cuts on the deposit energy in shower counter would be adjusted in such a way that the pion suppression efficiency was optimized to be the maximum while the electron acceptance efficiency was required to be above 99%.

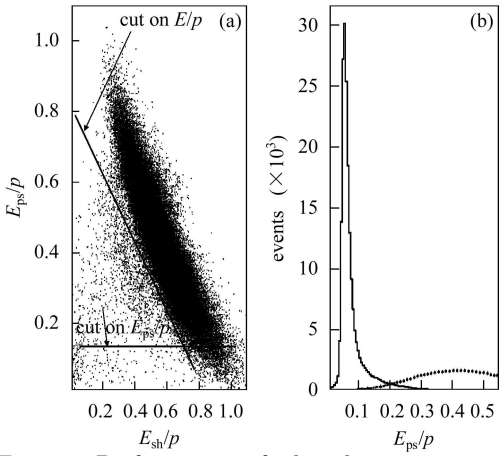

Fig. 3. Performance of the shower counter. (a) the scattering plot of electron sample; (b) $E_{\rm ps}/p$ for electron (error bars) and π (histogram).

The correlation between E/p cut and $E_{\rm ps}/p$ cut must be carefully handled. One had to avoid double counting those events dropped by two cuts. The E/p cut was adjusted until its inefficiency was about 0.5% firstly for an electron sample which was selected with a tight Cerenkov cut(here it was $1500 < \Sigma_{\rm ADC} < 2000$). Then this E/p cut was applied to the sample to count the events dropped by the pre-shower counter cut $E_{\rm ps}/p$. The $E_{\rm ps}/p$ cut was obtained while the inefficiency of the combined two cuts was less than 1%. The pion rejection could be obtained directly with the optimized shower cuts.

The performance of the shower counter cut was shown in Fig. 3.

2.3 PID cut and efficiency

The PID cuts in Cerenkov detector obtained from Fig. 2. As high $\varepsilon_{\rm e}^{\rm cer}$ and $\eta_{\pi}^{\rm cer}$ are required, the $\Sigma_{\rm ADC}$ can be selected to be higher than 350. The $\varepsilon_{\rm e}^{\rm cer}$ and $\eta_{\pi}^{\rm cer}$ with this cut are 99.68±0.10(stat.)% and 98.62±0.12(stat.)%, respectively.

The shower cuts are adjusted to $E/p>0.77$ and $E_{\rm ps}/p>0.095$. The electron acceptance efficiency $\varepsilon_{\rm e}^{\rm sh}$ and pion rejection $\eta_{\pi}^{\rm sh}$ of the optimized shower cuts are 99.07±0.11 (stat.)% and 99.05±0.13 (stat.)%, respectively.

Table 1. The optimized shower cuts and PID efficiency for different kinematic runs($\Sigma_{\rm ADC}>350$).

$E_{\rm bm}$	P_0	E/p	$E_{\rm ps}/p$	$\varepsilon_{\rm e}$(%)	η_{π}(%)
1.541	1.250	0.81	0.095	98.73±0.14	99.99±0.25
1.541	1.157	0.80	0.100	98.68±0.15	99.99±0.25
1.541	1.075	0.79	0.095	98.71±0.14	99.99±0.24
1.541	0.997	0.77	0.095	98.75±0.16	99.99±0.24
1.541	0.919	0.76	0.105	98.74±0.15	99.99±0.23
1.541	0.785	0.73	0.110	98.77±0.16	99.99±0.22
1.148	0.907	0.79	0.110	98.68±0.13	99.99±0.24
1.148	0.850	0.78	0.115	98.64±0.14	99.99±0.24
1.148	0.794	0.76	0.105	98.63±0.14	99.99±0.23
1.148	0.728	0.73	0.120	98.65±0.14	99.99±0.23
1.148	0.671	0.72	0.125	98.64±0.15	99.99±0.22
2.235	1.924	0.80	0.110	98.71±0.14	99.99±0.23
2.235	1.789	0.79	0.105	98.70±0.14	99.99±0.23
2.235	1.440	0.78	0.115	98.72±0.15	99.99±0.22
2.235	1.246	0.76	0.120	98.68±0.16	99.99±0.21
2.235	1.078	0.75	0.130	98.64±0.16	99.99±0.22
2.235	0.952	0.74	0.130	98.63±0.17	99.99±0.21
3.322	2.383	0.82	0.090	98.77±0.16	99.99±0.24
3.322	2.288	0.81	0.100	98.78±0.16	99.99±0.23
3.322	2.128	0.80	0.110	98.75±0.16	99.99±0.23

So the PID cut efficiency, the electron acceptance efficiency $\varepsilon_{\rm e}$ and the pion rejection η_{π}, could be calculated as:

$$\begin{aligned}\varepsilon_{\rm e}&=\varepsilon_{\rm e}^{\rm cer}\times\varepsilon_{\rm e}^{\rm sh}=98.75\pm0.16\%,\\ \eta_{\pi}&=1-(1-\eta_{\pi}^{\rm cer})\times(1-\eta_{\pi}^{\rm sh})=99.99\pm0.24\%.\end{aligned}\tag{3}$$

Because the width of E/p and $E_{\rm ps}/p$ depends on the kinematic of particles, the shower cuts should be optimized for different kinematic runs. Following the cut selection method mentioned before, the optimized shower cuts and the PID efficiency for all kinematic runs at GDH experiment have been obtained, which are shown in Table 1, where the $\Sigma_{\rm ADC}$ is required to be higher than 350.

The $E_{\rm bm}$, P_0 are the incident beam energy and the momentum of the scattering electron with GeV unit, respectively. The scattering angle is 6°.

3 Conclusion

The PID cut and its efficiency for the small angle GDH experiment have been optimized. Because of the dependence of the kinematic, 20 PID cuts are obtained for the responding runs. After the PID optimization, the electron acceptance efficiency is about 98.60±0.15 (stat.)%, the pion rejection is higher than 99.99±0.25 (stat.)%. The pion and low energy events can be rejected effectively by the gas Cherenkov detector and shower counter. The statistic is at a high level which can lead to a better uncertainty for the cross section and its asymmetry calculation. The systematic uncertainties, which mainly come from the resolution of detectors, are not included here.

We would like to thank J.P. Chen for his suggestion and V.Sulkosky, X.C. Zhen, K. Slifer for their advices.

References

1 Gerasimov S. Yaz., 1965, **2**: 598; Drell S D, Hearn A C. Phys. Rev. Lett., 1966, **16**: 908
2 Fermi E. Phys. Rev., 1940, **57**: 458
3 Alcorn J et al(JLab Collaboration). NIM, 2004, **A522**: 294
4 Iodice M. NIM, 1998, **A411**: 223
5 LÜ Hai-Jiang, YAN Xin-Hu, YE Yun-Xiu et al. HEP & NP, 2007, **31**(5): 492 (in Chinese)
(吕海江, 闫新虎, 叶云秀等. 高能物理与核物理, 2007, **31**(5): 492)
6 LÜ Hai-Jiang, JIANG Yi, YE Yun-Xiu et al. HEP & NP, 2007, **31**(1): 84—87 (in Chinese)
(吕海江, 蒋一, 叶云秀等. 高能物理与核物理, 2007, **31**(1): 84—87)

JLab Hall-A 上小角度GDH实验中的粒子鉴别及其效率*

吕海江[1,2;1)] 叶云秀[1] 闫新虎[1] 蒋一[1] 张沛[1] 叶秋健[1]

1 (中国科学技术大学近代物理系 合肥 230026)
2 (黄山学院物理系 黄山 245021)

摘要 在JLab的A大厅上的小角度GDH实验中, 因为散射截面及截面不对称度的测量需要干净的电子样本和足够的事例统计, 径迹在簇射量能器和气体阈契仑柯夫探测器理的信息被用来完成粒子鉴别的任务. 通过优化粒子在两种探测器里的信息筛选条件, 可以得到较高的电子接收效率和π的去除能力. 因为探测器的分辨能力与粒子的动量等运动学参量有关, 所以对于不同的数据的粒子鉴别条件分别进行了优化, 并得到了对应的电子接收效率和π的去除能力.

关键词 GDH求和规则 粒子鉴别 效率 优化

2007 – 01 – 04 收稿
* 国家自然科学基金 (10605022) 和安徽省教育厅自然科学基金 (KJ2007B028) 资助
1) E-mail: luhj9404@mail.ustc.edu.cn